# Thermodynamic Analysis of Catalysis by the Dihydroorotases from Hamster and *Bacillus caldolyticus*, As Compared with the Uncatalyzed Reaction†

Danny T. Huang,‡ Jacob Kaplan,§ R. Ian Menz,|| Vittorio L. Katis,⊥ R. Gerry Wake,§ Feng Zhao,# Richard Wolfenden,# and Richard I. Christopherson*,§

*School of Molecular and Microbial Biosciences, University of Sydney, Sydney, New South Wales 2006, Australia, and Department of Biochemistry and Biophysics, University of North Carolina, Chapel Hill, North Carolina 27599-7260*

*Received March 26, 2006; Revised Manuscript Received May 8, 2006*

ABSTRACT: Dihydroorotase (DHOase, EC 3.5.2.3) from the extreme thermophile *Bacillus caldolyticus* has been subcloned, sequenced, expressed, and purified as a monomer. The catalytic properties of this thermophilic DHOase have been compared with another type I enzyme, the DHOase domain from hamster, to investigate how the thermophilic enzyme is adapted to higher temperatures. *B. caldolyticus* DHOase has higher $V_{max}$ and $K_s$ values than hamster DHOase at the same temperature. The thermodynamic parameters for the binding of L-dihydroorotate were determined at 25 °C for hamster DHOase ($\Delta G = -6.9$ kcal/mol, $\Delta H = -11.5$ kcal/mol, $T\Delta S = -4.6$ kcal/mol) and *B. caldolyticus* DHOase ($\Delta G = -5.6$ kcal/mol, $\Delta H = -4.2$ kcal/mol, $T\Delta S = +1.4$ kcal/mol). The smaller enthalpy release and positive entropy for thermophilic DHOase are indicative of a weakly interacting Michaelis complex. Hamster DHOase has an enthalpy of activation of 12.3 kcal/mol, similar to the release of enthalpy upon substrate binding, rendering the $k_{cat}/K_s$ value almost temperature independent. *B. caldolyticus* DHOase shows a decrease in the enthalpy of activation from 12.2 kcal/mol at temperatures from 30 to 50 °C to 5.3 kcal/mol for temperatures of 50−70 °C. Vibrational energy at higher temperatures may facilitate the transition ES → ES‡, making $k_{cat}/K_s$ almost temperature independent. The pseudo-first-order rate constant for water attack on L-dihydroorotate, based on experiments at elevated temperature, is $3.2 \times 10^{-11}$ s$^{-1}$ at 25 °C, with $\Delta H^{‡} = 24.7$ kcal/mol and $T\Delta S^{‡} = -6.9$ kcal/mol. Thus, hamster DHOase enhances the rate of substrate hydrolysis by a factor of $1.6 \times 10^{14}$, achieving this rate enhancement almost entirely by lowering the enthalpy of activation ($\Delta\Delta H^{‡} = -19.5$ kcal/mol). Both the rate enhancement and transition state affinity of hamster DHOase increase steeply with decreasing temperature, consistent with the development of H-bonds and electrostatic interactions in the transition state that were not present in the enzyme−substrate complex in the ground state.

Dihydroorotase (DHOase)[1] catalyzes the reversible cyclization of *N*-carbamyl-L-aspartate (CA-asp) to L-dihydroorotate (DHO) in the third reaction of the pathway for de novo biosynthesis of pyrimidine nucleotides. In prokaryotes, the enzyme is monofunctional, while in higher eukaryotes, it is part of a trifunctional protein called CAD, that contains the first three enzymes of the pyrimidine pathway in the sequence $H_3N^+$−CPSase−DHOase−bridge−ATCase−$COO^-$ (*1*−*3*). Phylogenetic analysis of amino acid sequences of DHOases shows two types that share a common ancestor with other amidohydrolases (*4*). Type I DHOases are larger (∼45 kDa), may contain one zinc ion at the active site, and include the DHOase domain from trifunctional CAD (*5*) and the monofunctional enzymes from *Bacillus caldolyticus* (studied here) and *Aquifex aeolicus* for which there is a three-dimensional structure (*6*). Type II DHOases are smaller (∼38 kDa) and contain two zinc ions at the active site, bridged by a carboxylated lysine residue, exemplified by the DHOases from *Clostridium oroticum* (*7*) and *Escherichia coli* for which there is a three-dimensional structure (*8*, *9*).

The crystallographic structure of the type I DHOase from *A. aeolicus* shows a single zinc atom bound by two histidine residues, an aspartate, and a hydroxide ion derived from a water molecule (*6*). A similar arrangement with a single zinc coordinated by three histidines was proposed for the DHOase domain of CAD from hamster (see Figure 4 of ref *10*). With DHO bound at the active site, the oxygen of the C6 ring carbonyl group interacts with the zinc, polarizing the C═O

† This work was supported by the Australian National Health and Medical Research Council, Project Grant 253781.

* To whom correspondence should be addressed. Phone: 61-2-9351-6031. Fax: 61-2-9351-4726. E-mail: ric@mmb.usyd.edu.au. URL: http://www.mmb.usyd.edu.au.

‡ Present address: Department of Structural Biology and Genetics/Tumor Cell Biology, St. Jude's Children's Research Hospital, Memphis, TN 38105.

§ University of Sydney.

|| Present address: School of Biological Sciences, Flinders University of South Australia, GPO Box 2100, Adelaide, SA 5001, Australia.

⊥ Present address: Department of Biochemistry, University of Oxford, South Parks Road, Oxford OX1 3QU, U.K.

# University of North Carolina.

[1] Abbreviations: CA-asp, *N*-carbamyl-L-aspartate; CAD, the trifunctional protein containing carbamyl phosphate synthetase (CPSase, EC 2.7.2.9), aspartate transcarbamylase (ATCase, EC 2.1.3.2), and dihydroorotase (DHOase, EC 3.5.2.3); DHO, L-dihydroorotate; DTNB, 5,5′-dithiobis(2-nitrobenzoic acid); HDDP, 2-oxo-1,2,3,6-tetrahydropyrimidine-4,6-dicarboxylic acid; hDHOase, hamster DHOase domain; BcDHOase, thermophilic DHOase from *Bacillus caldolyticus*; TCEP, tris(2-carboxyethyl)phosphine hydrochloride; TNB, thiobis(2-nitrobenzoic acid).

10.1021/bi060595w CCC: $33.50 
Published on Web 06/15/2006

bond, and the coordinated hydroxide attacks the C6 carbonyl carbon. Concurrently, the proton on the hydroxide transfers to another aspartate residue at the active site, and a tetrahedral intermediate, approaching the transition state in structure, with two oxygen atoms at C6 forms an inner-sphere coordination complex with the zinc. The proton on the aspartate residue is transferred to N3 of the transition state that then collapses with C−N bond scission. The importance of an active site aspartate residue (D230 of hDHOase) in catalysis has been tested and established by site-directed mutagenesis (*10*). The conservative mutation D230E yielded a mutant hDHOase with a $K_s$ for DHO increased 14-fold and a $V_{max}$ reduced by 0.063-fold. The mutant enzymes D230G and D230N were catalytically inactive. Thus, D230 is involved in both binding and catalysis.

In this paper, the thermodynamics of catalysis of the reverse reaction DHO → CA-asp have been analyzed for the type I DHOases from hamster and *B. caldolyticus*. The DHOase from *B. caldolyticus* has been subcloned, expressed, and purified. The effects of temperature and inhibition of these DHOases have been studied to gain a better understanding of substrate binding and catalysis at pH 8.0 where the enzyme has maximal activity for the reverse reaction, DHO → CA-asp (*11*). To analyze the proficiency of DHOase as a catalyst, and its effects on the enthalpy and entropy of substrate activation, we also examined the effects of changing pH and temperature on the rate of DHO hydrolysis in water, in the absence of a catalyst.

## EXPERIMENTAL PROCEDURES

*Materials and Methods*. All water used was purified by reverse osmosis followed by passage through a Millipore reagent water system (Millipore Co., Bedford, MA) to give a resistance of 18 MΩ. L-[2-$^{14}$C]Dihydroorotate was synthesized as described previously (*15*). Tris(2-carboxyethyl)-phosphine hydrochloride (TCEP) was from Pierce (Rockford, IL). Factor Xa was from Novagen Inc. (Madison, WI). Ni-NTA agarose resin was from Qiagen Pty Ltd. (Victoria, Australia). The Poros Q anion-exchange column was from Perseptive Biosystems (Foster City, CA). 5,5′-Dithiobis(2-nitrobenzoic acid) (DTNB) was from Sigma Chemical Co. (St. Louis, MO). 2-Oxo-1,2,3,6-tetrahydropyrimidine-4,6-dicarboxylic acid (HDDP) was synthesized as described previously (*15*).

*Cloning of Dihydroorotase from B. caldolyticus (BcDHOase)*. The gene, *pyrC*, encoding DHOase from *B. caldolyticus* was amplified by PCR from a plasmid, pSY18, containing *pyrB* and *pyrC*, provided by Dr. J. Neuhard [University of Copenhagen, Denmark (*12*)] with a forward primer that introduced a factor Xa cleavage site. The PCR product was cloned into the expression vector pETMCSIII, which adds a hexahistidine tail to the N-terminus of the expressed protein. The resulting plasmid was used to transform *E. coli* BL21(DES/pLysS).

*Mass Spectroscopy*. Samples were applied to a Jupiter 5 μm C18 column (Phenomenex, Torrance, CA) and eluted with a gradient of acetonitrile in 0.1% (v/v) acetic acid and 0.02% (v/v) TFA at a flow rate of 0.25 mL/min. The eluate was analyzed by electrospray ionization mass spectrometry using a Thermoquest LCQ classic mass spectrometer (Thermoquest, San Jose, CA).

*Overexpression and Purification of BcDHOase*. The recombinant strain of *E. coli* was grown in L-broth containing ampicillin (100 μg/mL), chloramphenicol (25 μg/mL), and zinc chloride (0.1 mM) at 37 °C. When the absorbance at 600 nm was ∼0.8, the cells were induced with IPTG (250 μM) for 3 h, harvested, and lysed in buffer containing 20 mM Na·Hepes (pH 7.5), 0.1 mM EDTA, 133 μM PMSF, leupeptin (2 μg/mL), and pepstatin A (1 μg/mL). After centrifugation (39000*g*, 30 min, 4 °C), the soluble fraction was applied to a Ni-NTA agarose column (1 × 5 cm) and washed with a step gradient of imidazole at 10, 20, and 40 mM in 20 mM sodium phosphate buffer (pH 7.6) and 300 mM NaCl. The hexahistidine-tagged BcDHOase was eluted with 250 mM imidazole and further purified on a Poros Q column eluted with a 0−1.0 M NaCl gradient in 20 mM Na·Hepes (pH 7.5). The hexahistidine tag was cleaved by incubating the tagged BcDHOase (0.2−1.0 mg/mL) with factor Xa (1 unit cleaves 200 μg of protein) in 20 mM Na·Hepes (pH 7.5), 100 mM NaCl, and 2 mM $CaCl_2$ at 18 °C for 3−4 days. The cleaved BcDHOase was separated from the tagged precursor by Ni-NTA chromatography (see above) and stored in 20 mM Na·Hepes (pH 7.5) at 4 °C.

*Gel Filtration of BcDHOase*. Tagged BcDHOase after purification on a Ni-NTA column was analyzed by chromatography on a Sephadex G-75 column (1.0 × 40 cm; Amersham Pharmacia Biotech, Uppsala, Sweden) eluted with 20 mM Na·Hepes (pH 7.5) and 0.3 M NaCl. Fractions were assayed for DHOase activity and analyzed by native gel electrophoresis and SDS−PAGE.

*Preparation of Recombinant Hamster Dihydroorotase*. *E. coli* K strain SØ1263/*pyrC*$^-$, transformed with the plasmid pCW25, encoding the hamster DHOase domain with an extra 33 amino acid residues extending into the bridge region (hDHOase), was grown and induced with IPTG as previously described (*38*). hDHOase was purified from cell lysates by chromatography on N-linked butylamine−agarose and DEAE-Sephacel (*38*). Pure hDHOase was stored in 20 mM Na·Hepes (pH 7.3), 10% (v/v) glycerol, 0.1 mM EDTA, and 1 mM DTT at −20 °C.

*Analysis for Disulfide Bonds*. The number of free cysteines and disulfide bonds in hDHOase and BcDHOase was determined by titration with 5,5′-dithiobis(2-nitrobenzoic acid) (DTNB). Incubation mixtures contained DHOase (10 nmol) in 50 mM Na·Hepes (pH 7.4) in the presence or absence of 6 M guanidine hydrochloride. The reaction was initiated by addition of DTNB (0.15 mM), and the absorbance at 412 nm was monitored to a constant value. The number of free cysteine(s) was calculated using $\epsilon_{412nm}$($NTB^-$ ion) = 14150 M/cm, or 13700 M/cm in the presence of guanidine hydrochloride (*39*).

*Dependence of Enzyme Kinetics on Temperature*. DHOase was assayed in the degradative direction (DHO → CA-asp) as described previously (*15*). Reaction mixtures (23 μL) containing 50 mM Na·Hepes (pH 8.0), 5% (v/v) glycerol, and L-[2-$^{14}$C]DHO (0−400 μM for hDHOase; 0−1000 μM for BcDHOase) were preincubated at various temperatures (25−50 °C for hDHOase; 25−90 °C for BcDHOase) for 3 min. Reactions were initiated by adding pure DHOase (2 μL; 2−10 ng for hDHOase and 0.4−2 ng for BcDHOase), less than 15% of the [2-$^{14}$C]DHO was consumed during the assay, and aliquots (6 μL) were spotted onto poly(ethylenimine)−cellulose chromatograms at 3, 6, and 9 min. Reaction

velocities for CA-asp formation were determined by linear regression to these three time points. $V_{max}$ and $K_s$ values at various temperatures were calculated by nonlinear regression of data at 10 DHO concentrations to the Michaelis−Menten equation using Sigma-Plot (Jandel Scientific, Corte Madera, CA).

*Competitive Inhibition.* The interactions of the competitive inhibitor HDDP (*10*, *15*) with hDHOase and BcDHOase were compared. Reaction mixtures (23 $\mu$L) contained 50 mM Na·Hepes (pH 8.0), 5% (v/v) glycerol, and L-[2-$^{14}$C]DHO (concentration 5-fold $K_s$) with varying concentrations of HDDP (0−100 $\mu$M for hDHOase; 0−400 $\mu$M for BcDHOase), and the reaction was initiated by addition of DHOase (2 $\mu$L). The reaction was assayed at 37 °C (hDHOase and BcDHOase) and 60 °C (BcDHOase). $K_i$ values for competitive inhibition of DHOase by HDDP were determined by fitting the data to eq 1, where $v$ is the measured initial rate, $V$ is the maximal rate, $S$ is the DHO concentration, $I$ is the inhibitor concentration, $K_s$ is the dissociation constant for DHO, and $K_i$ is the inhibition constant.

$$v = \frac{VS}{(1 + I/K_i)K_s + S} \tag{1}$$

*Analysis of Thermodynamic Parameters*. For the reaction catalyzed by DHOase, it is assumed that catalysis is the rate-limiting step and that all enzyme species are in rapid equilibrium; i.e., $K_s = K_m$. This assumption is substantiated by a recent study of the $^{13}$C and $^{15}$N isotope effects for the conversion of DHO → CA-asp using hDHOase and BcDHOase (M. A. Anderson, W. W. Cleland, D. T. Huang, C. Chan, M. Shojaei, and R. I. Christopherson, manuscript submitted for publication). The results indicated that the chemistry of the DHOase reaction is at least partially rate-limiting for hDHOase and BcDHOase.

The enzymic conversion of DHO → CA-asp can be described as

$$E + S \underset{K_s}{\overset{K_{eq}}{\rightleftharpoons}} ES \rightarrow ES^{\ddagger} \rightarrow E + P \tag{2}$$

The standard free energy change for formation of the ES complex is given by

$$\Delta G^\circ = -2.303RT \log K_{eq} \tag{3}$$

$K_{eq} = 1/K_s$; thus eq 3 can be written as

$$\Delta G^\circ = 2.303RT \log K_s \tag{4}$$

and

$$\Delta G^\circ = \Delta H^\circ - T\Delta S^\circ \tag{5}$$

where $\Delta H^\circ$ is the standard enthalpy change, $\Delta S^\circ$ is the standard entropy change, and $R$ is the gas constant (1.98 cal mol$^{-1}$ K$^{-1}$). Combining eqs 4 and 5 we obtain

$$\log K_s = \frac{\Delta H^\circ}{2.303RT} - \frac{\Delta S^\circ}{2.303R} \tag{6}$$

A plot of log $K_s$ versus $1/T$ would give $\Delta H^\circ$ for the association, E + S → ES. The $\Delta G^\circ$ for the association can be calculated from eq 4 and hence $\Delta S^\circ$ from eq 5 (*13*).

The standard free energy of activation, ES → ES$^{\ddagger}$, is given by

$$\Delta G^{\ddagger} = -2.303RT \log \frac{k_{cat}h}{k_B T} \tag{7}$$

and

$$\Delta G^{\ddagger} = \Delta H^{\ddagger} - T\Delta S^{\ddagger} \tag{8}$$

where $h$ is Planck's constant (6.624 × 10$^{-27}$ erg s), $k_B$ is the Boltzmann constant (1.38 × 10$^{-16}$ erg K$^{-1}$), and $k_{cat}$ is the rate constant for the rate-limiting step of catalysis. $\Delta H^{\ddagger}$ is the enthalpy of activation, and $\Delta S^{\ddagger}$ is the entropy of activation. Combining eqs 7 and 8 we obtain

$$\log \frac{k_{cat}}{T} = -\frac{\Delta H^{\ddagger}}{2.303RT} + \log \frac{k_B}{h} + \frac{\Delta S^{\ddagger}}{2.303R} \tag{9}$$

A plot of log($k_{cat}/T$) versus $1/T$ enables determination of $\Delta H^{\ddagger}$ from the slope. $\Delta G^{\ddagger}$ can be determined from eq 7 and hence $\Delta S^{\ddagger}$ from eq 8 (*40*).

*Circular Dichroism Spectroscopy*. Experiments were carried out with a Jasco J-720 spectropolarimeter, and all CD spectra were obtained at 20 °C in a 0.1 cm path length quartz cell. Protein samples (0.1−0.2 mg/mL) were in 10 mM potassium phosphate, pH 7.4. For thermal denaturation experiments, the temperature of a water bath was increased by 1 °C/min. Ellipticity was monitored at 194 nm under reducing conditions (5 mM TCEP). For urea unfolding experiments, protein samples (0.2 mg/mL) in urea (0−8 M) under reducing conditions (5 mM TCEP) were monitored for 3 min at 222 nm, and a mean ellipticity was obtained. An aliquot of hDHOase or BcDHOase was removed and kept on ice after treatment with urea. The DHOase activities were then measured at 37 °C as described earlier. The ability for hDHOase and BcDHOase to refold after denaturation by urea was analyzed by diluting protein samples treated with urea (6 M for hDHOase and 8 M for BcDHOase) for 10 min, 10-fold with 10 mM potassium phosphate, pH 7.4, and 5 mM TCEP. Control protein samples (0.02 mg/mL) with or without urea (6 M for hDHOase and 8 M for BcDHOase) were used. CD spectra were obtained and ellipticities at 222 nm were compared to yield percentage of refolding. Both hDHOase and BcDHOase cannot be refolded after prolonged incubation with high concentration of urea.

$\Delta G_u^{H_2O}$, the $\Delta G$ for unfolding at zero denaturant concentration, was determined by fitting data to the equation (*14*)

$$\Delta G_u = \Delta G_u^{H_2O} - m[\text{urea}] \tag{10}$$

where $m$ is a measure of the dependence of $\Delta G_u$ on denaturant concentration. The urea concentration required for unfolding 50% of protein, $[\text{urea}]_{1/2}$, is given by

$$[\text{urea}]_{1/2} = \Delta G_u^{H_2O}/m \tag{11}$$

*Uncatalyzed Hydrolysis of DHO*. In a typical experiment, samples of DHO (0.01 M) dissolved in buffer (potassium [$^2$H]formate, [$^2$H$_3$]acetate, phosphate, borate, or carbonate, 0.1 M) were sealed under vacuum in quartz tubes and heated for timed intervals in a Thermolyne 47900 furnace between 99 and 167 °C. After cooling, the tube's contents were diluted

with $^2H_2O$ to which pyrazine had been added as an integration standard for analysis by proton NMR. Apparent first-order rate constants for reaction were determined from the integrated intensities of carbon-bound protons (t 4.07 ppm, 5-H; d 2.91 and d 2.75 ppm, 6-H) of the substrate remaining, plotted as a semilogarithmic function of time. Similar results were obtained using ninhydrin to follow the course of the reaction.

## RESULTS

*Characterization of BcDHOase.* The gene encoding DHOase from the extreme thermophile *B. caldolyticus* was cloned from the plasmid pSY18 (*12*) into pETMCSIII and overexpressed in *E. coli* BL21/pLysS. In contrast to the published sequence (*12*), analysis of several independent clones showed an extra GAG codon (underlined) between base pairs 1410 and 1411 [using numbering from pSY18 (*12*)] or 126 bp from the 5′-end of the gene, making the amino acid sequence Ala39-Asn40-Glu41-Glu42-Asp43. Mass spectroscopy showed that BcDHOase with the hexahistidine tag has a molecular weight of 48085.1 ± 1.4 compared with a calculated molecular weight (including Glu42) of 48085.53. The tagged BcDHOase contained approximately 1.0 zinc atom per subunit measured by atomic absorption spectroscopy, consistent with a type I DHOase as proposed by Fields et al. (*4*).

Tagged BcDHOase was purified by chromatography on a Ni-NTA column, followed by a Poros Q anion-exchange column. Pure tagged BcDHOase eluted from a Sephadex G-75 column after the void peak, consistent with monomeric BcDHOase (48 kDa). The 6×His-tagged BcDHOase had the MHHHHHHSSGHIEGR↓ start sequence at the N-terminus with the proposed factor Xa cleavage site at the arrow. The tagged precursor DHOase ($M_r$ = 48085) was digested with factor Xa to yield a product ($M_r$ 46915) corresponding to the SGHIEGR start sequence at the N-terminus determined by mass spectrometric analysis. It appears that the N-terminus may be buried preventing cleavage at the engineered factor Xa site. Subsequent studies have shown that the BcDHOase with the full tag, seven amino acid partial tag, or the wild-type enzyme has identical catalytic properties. BcDHOase contains seven cysteine residues; titration with DTNB showed three disulfide bonds and one buried cysteine. hDHOase has six cysteines; DTNB titration showed one disulfide bond, three buried cysteines, and one exposed cysteine.

*Effects of Temperature on Catalysis.* $V_{max}$ and $K_s$ values for hDHOase and BcDHOase at pH 8.0 were determined at temperatures from 25 to 50 °C and 25−70 °C, respectively. A plot of log $K_s$ versus $1/T$ was used to determine $\Delta H°$ for substrate binding, E + S → ES (Figure 1), and $\Delta G°$ and $\Delta S°$ were determined from eqs 4 and 5. A plot of $\log(k_{cat}/T)$ versus $1/T$ was used to determine $\Delta H^‡$, the enthalpy of activation (ES → ES$^‡$, Figure 2); the other thermodynamic activation parameters, $\Delta G^‡$ and $\Delta S^‡$, were then determined from eqs 7 and 8. Values for these parameters are listed in Table 1. The contributions of enthalpy and entropy to $\Delta G°$ for formation of the Michaelis complex (E + S → ES) are different for hDHOase and BcDHOase. BcDHOase has a positive entropy ($T\Delta S°$) for binding of DHO while hDHOase has entropy loss with a higher release of enthalpy (Table 1).

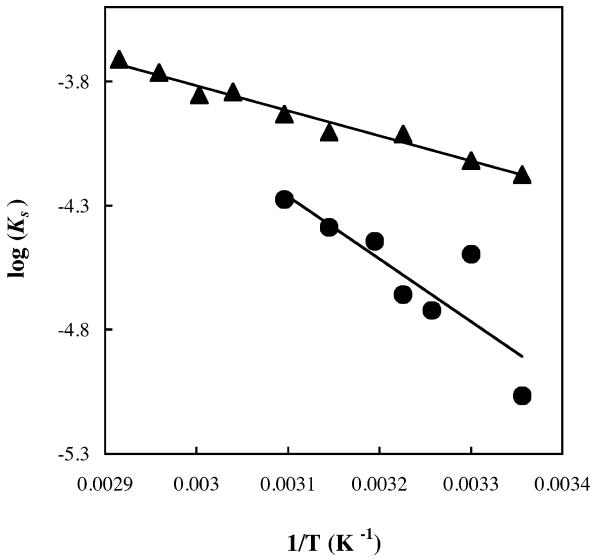


FIGURE 1: Effect of temperature on the binding of DHO to DHOases. $K_s$ values for DHO were determined at the indicated temperatures and data analyzed as described in Experimental Procedures. Key: (●) hDHOase; (▲) BcDHOase.

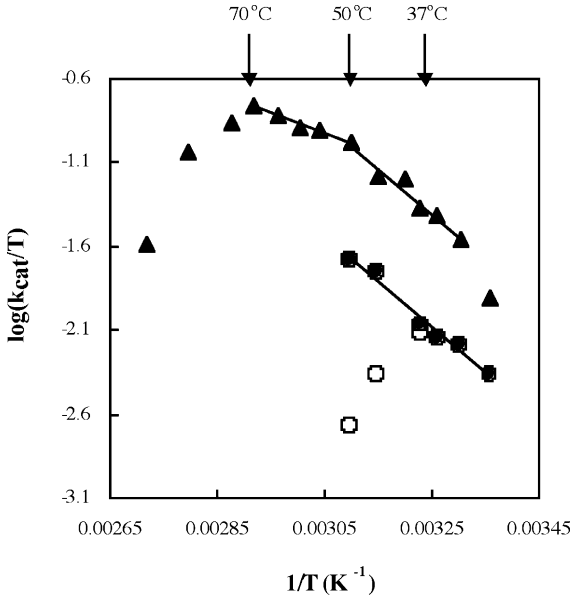


FIGURE 2: Plot of $\log(k_{cat}/T)$ versus $1/T$ for DHOases. $V_{max}$ values were determined at the indicated temperatures as described in Experimental Procedures. Preincubation of hDHOase at reaction temperatures greater than 37 °C for 10 min prior to assay resulted in a decrease in activity (○). The kinetic parameters obtained for hDHOase at temperatures greater than 37 °C up to 50 °C were determined in less than 10 min. Key: (●) hDHOase; (▲) BcDHOase.

The plot of $\log(k_{cat}/T)$ versus $1/T$ (Figure 2) shows two different slopes for BcDHOase in the ranges 30−50 °C and 50−70 °C, yielding enthalpies of activation ($\Delta H^‡$) of 12.2 and 5.3 kcal/mol, respectively. The former is similar to that for hDHOase. BcDHOase could have an even higher enthalpy of activation at temperatures below 30 °C (Figure 2). At higher temperatures, BcDHOase exhibits a more negative value for $T\Delta S^‡$ (Table 1), due to increased ordering of the protein and/or solvent water in passing from the ground state to the transition state. For both enzymes, the $V_{max}$ and $K_s$ values increase with increasing temperature. BcDHOase has higher $V_{max}$ and $K_s$ values at a particular temperature

Table 1: Comparison of Kinetic and Thermodynamic Parameters for DHO Hydrolysis by DHOases from Hamster and *B. caldolyticus*

| parameter | hDHOase | BcDHOase |
|---|---|---|
| $V_{max}$ ($\mu$mol min$^{-1}$ mg$^{-1}$)[a] | 3.9 ± 0.5 | 77.4 ± 4.5 |
| $K_s$ ($\mu$M)[a] | 22 ± 4.7 | 195 ± 28 |
| $k_{cat}/K_s$ (s$^{-1}$ M$^{-1}$)[a] | 18300 | 31800 |
| $E_a$ (kcal/mol)[b] | 12.9 ± 0.9 (25−50 °C) | 12.8 ± 1.2 (30−50 °C)<br>6.0 ± 0.4 (50−70 °C) |
| $\Delta H^{\ddagger}$ (kcal/mol) | 12.3 ± 0.9 (25−50 °C) | 12.2 ± 1.2 (30−50 °C)<br>5.3 ± 0.4 (50−70 °C) |
| $T\Delta S^{\ddagger}$ (kcal/mol) | −5.0 to −5.4 (25−50 °C)[c] | −4.3 to −4.5 (30−50 °C)[c]<br>−11.7 to −12.1 (50−70 °C)[c] |
| $\Delta G^{\ddagger}$ (kcal/mol) | 17.3−17.7 (25−50 °C)[c] | 16.5−16.7 (30−50 °C)[c]<br>16.7−17.4 (50−70 °C)[c] |
| $\Delta H°$ (kcal/mol)[d] | −11.5 ± 3.1 | −4.2 ± 0.8 |
| $T\Delta S°$ (kcal/mol)[d] | −4.6 | +1.4 |
| $\Delta G°$ (kcal/mol)[d] | −6.9 | −5.6 |

[a] Kinetic parameters were measured at pH 8.0, 37 °C for hDHOase and 70 °C for BcDHOase. [b] $E_a$ was determined from the plot of log $k_{cat}$ versus $1/T$ where slope = $-E_a/2.303R$. [c] Two values were calculated from eqs 7 and 8 in Experimental Procedures using the indicated lower and upper temperatures. [d] $\Delta G°$, $\Delta H°$, and $\Delta S°$ are values for the association E + S → ES, where S is DHO. $\Delta G°$ and $\Delta S°$ were determined using eqs 4 and 5, respectively, at 25 °C.

compared with hDHOase. Figure 2 shows that BcDHOase has optimal activity at 70 °C similar to the optimal growth temperature of *B. caldolyticus* [72 °C (*12*)], while the optimum for hDHOase is approximately 37 °C. hDHOase was assayed at temperatures up to 50 °C where the enzyme remained stable for 10 min. At the optimum temperature of 70 °C, BcDHOase has a higher $k_{cat}/K_s$ value compared with hDHOase at 37 °C (Table 1).

*Thermal Denaturation.* BcDHOase started to unfold at temperatures greater than 70 °C with a $T_m$ of 79.5 °C monitored by circular dichroism (ellipticity at 194 nm, Figure 3). Increasing temperature induced a significant reduction in the ellipticity at 194 nm; there was little change from 200 to 230 nm, but two minima at 208 and 222 nm disappeared, with a new minimum formed at 216 nm. We were unable to obtain a definitive melting curve for hDHOase possibly due to protein aggregation upon unfolding, but there was a gradual decline in ellipticity above 40 °C (data not shown). Comparison of CD spectra of hDHOase at 20 and 90 °C showed a marked reduction in ellipticity at 190−200 nm at high temperature. Using the hamster DHOase domain obtained from limited digestion of CAD with elastase, Hemmens and Carrey (*13*) found a sharp transition at 45 °C measured by circular dichroism at 222 nm. The recombinant hDHOase domain used here contains an additional 33 amino acid residues on the C-terminus extending into the bridge region between the DHOase and ATCase domains. Thermal denaturation was irreversible for hDHOase and BcDHOase. The loss of enzymic activity observed at higher temperatures for the two DHOases coincided with loss of secondary structure indicated by decreases in ellipticity (Figure 3).

*Denaturation with Urea.* Figure 4 shows denaturation of hDHOase and BcDHOase by increasing concentrations of

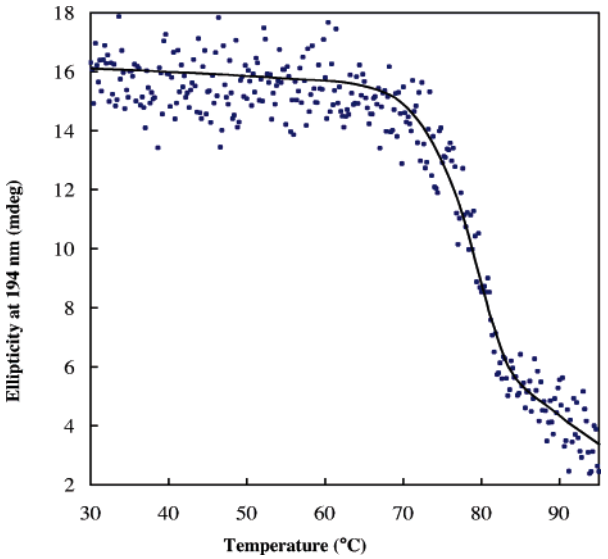


FIGURE 3: Thermal denaturation curve for BcDHOase. Protein (0.17 mg/mL) in 10 mM sodium phosphate, pH 7.4, and 5 mM TCEP was monitored by circular dichroism at 194 nm with a ramp rate of 1 °C/min.

urea under reducing conditions, monitored by circular dichroism at 222 nm and enzymic activity at 37 °C. The concentration of urea for half-maximal unfolding of BcDHOase, $[urea]_{1/2}$, was 5.7 ± 0.5 M; the *m*-value was 1.39 ± 0.09 kcal mol$^{-1}$ M$^{-1}$, determined from a two-state model of denaturation (*14*) by fitting the data to eqs 9 and 10. The $\Delta G_u^{H_2O}$ for unfolding is 7.94 ± 0.5 kcal/mol. The decrease in enzymic activity coincided with the unfolding of BcDHOase by urea with half-maximal activity at a urea concentration of ~5.7 M (Figure 4). Experimental data for hDHOase were not consistent with a two-state model. The first transition for denaturation of hDHOase in urea ($[urea]_{1/2}$ ~ 3.8 M) corresponded to the loss of enzymic activity (half-maximal activity at a urea concentration of ~3.3 M), and the second transition could indicate a change in aggregation state of the enzyme. The denaturation was partially reversible; the initial circular dichroism of hDHOase and BcDHOase was recovered to 70% and 75%, respectively. The activity of hDHOase was not recovered from urea concentrations of greater than 7 M. The data of Figure 4 show that BcDHOase is more resistant to unfolding by urea than hDHOase.

*Inhibition by HDDP.* A transition-state analogue inhibitor, HDDP (*10*, *15*), was tested against hDHOase and BcDHOase, and $K_i$ values were determined (Table 2). At 37 °C, hDHOase binds HDDP ($K_i$ = 4.5 $\mu$M) more tightly than DHO ($K_s$ = 22 $\mu$M), while BcDHOase binds HDDP ($K_i$ = 83 $\mu$M) only slightly more strongly than DHO ($K_s$ = 97 $\mu$M). This relationship between dissociation constants is similar at 60 °C for BcDHOase for HDDP ($K_i$ = 102 $\mu$M) compared with DHO ($K_s$ = 140 $\mu$M, Table 2). Preincubation of the enzyme with HDDP for 15 min at 37 or 60 °C prior to assay had no effect on the degree of inhibition.

*Spontaneous Hydrolysis of DHO.* Samples of DHO (0.01 M) were dissolved in potassium [$^2H_3$]acetate buffer (pH 4.0 at 25 °C, 0.1 M), sealed under vacuum in quartz tubes, and heated for timed intervals at various temperatures between 99 and 167 °C in a Thermolyne 47900 furnace. When the disappearance of DHO was monitored by proton NMR, its hydrolysis was found to proceed with first-order kinetics.

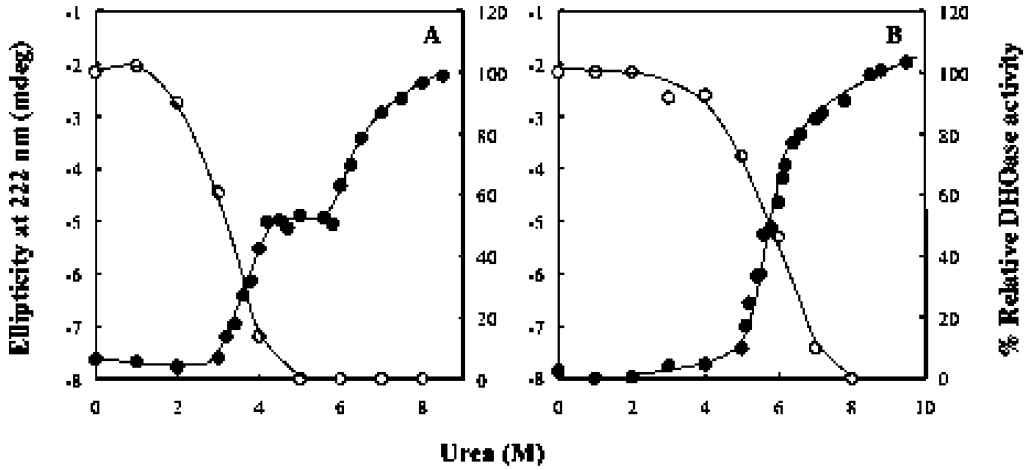


FIGURE 4: Denaturation of DHOase with urea. Samples of enzyme (0.2 mg of protein/mL) were incubated in the indicated urea concentrations in 10 mM sodium phosphate, pH 7.4, and 5 mM TCEP at 20 °C for 30 min. Enzymic activities of samples were measured at 37 °C immediately after analysis by circular dichroism. Key: (A) hDHOase; (B) BcDHOase; (●) circular dichroism at 222 nm; (○) enzymic activity.

Table 2: Dissociation Constants for Interaction of DHO and HDDP with HDHOase and BcDHOase[a]

| | $K_s$ ($\mu$M) | $K_i$ ($\mu$M) | $K_s/K_i$ |
|---|---|---|---|
| hDHOase (37 °C) | 22 ± 4.7 | 4.5 ± 0.7 | 4.9 |
| BcDHOase (37 °C) | 97 ± 39 | 83 ± 9 | 1.17 |
| BcDHOase (60 °C) | 140 ± 38 | 102 ± 4 | 1.37 |

[a] $K_s$ values were obtained from nonlinear regression of reaction velocities at ten different DHO concentrations to the Michaelis−Menten equation. $K_i$ values were obtained from Dixon plots at eight different HDDP concentrations with 100 $\mu$M [2-$^{14}$C]DHO for hDHOase and 500 and 750 $\mu$M [2-$^{14}$C]DHO for BcDHOase at 37 and 60 °C, respectively. Data were fitted by nonlinear regression to eq 1.

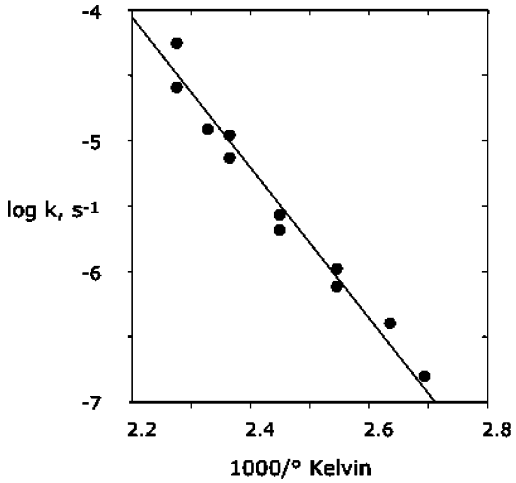


FIGURE 5: Rate constants observed for the hydrolysis of DHO (0.01 M) in potassium [$^2$H]acetate buffer (0.1 M, pH 4.0) plotted as a logarithmic function of reciprocal temperature (kelvin).

The results yielded a linear Arrhenius plot (Figure 5) with an extrapolated rate constant of $3.2 \times 10^{-11}$ $M^{-1}$ $s^{-1}$ at 25 °C. Extrapolation of the results of similar experiments conducted in other buffers (HCl, potassium [$^2$H]formate, phosphate, borate, or carbonate, 0.1 M) yielded values indicating that this reaction, like other reactions of carboxylic acid amides, is subject to specific acid and base catalysis but is uncatalyzed at pH 4 (Figure 6). We infer that the extrapolated rate constant of $3.2 \times 10^{-11}$ $M^{-1}$ $s^{-1}$ at 25 °C represents the pseudo-first-order rate constant for water attack on DHO, based on unit water activity. The thermodynamics

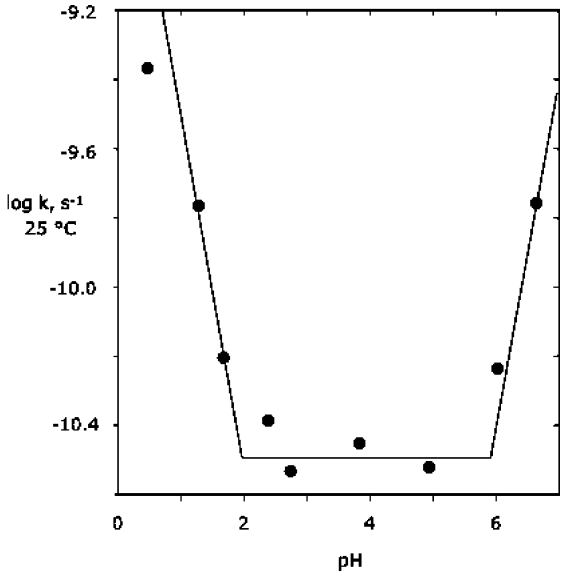


FIGURE 6: Rate constants for the hydrolysis of DHO (0.01 M), obtained by extrapolation to 25 °C of Arrhenius plots as in Figure 1, plotted as a function of pH in buffers containing 0.1 M HCl, potassium formate, potassium acetate, and potassium phosphate.

of activation for this reaction are $\Delta G^{\ddagger} = 30.7$ kcal/mol, $\Delta H^{\ddagger} = 24.7$ kcal/mol, and $T\Delta S^{\ddagger} = -6.9$ kcal/mol.

## DISCUSSION

Most type I and II DHOases from different species exist as dimers (*5*, *16*−*18*), but the enzymes from *Plasmodium berghei* and *Crithidia fasciculata* are monomeric (*19*). The overexpressed BcDHOase from *B. caldolyticus* investigated here is predominately monomeric. Dilution of *E. coli* DHOase can lead to an unstable hyperactive monomer (*20*), but the monomeric BcDHOase is stable during 6 months storage at 4−10 °C. The monomeric form of BcDHOase could be an adaptation by this organism to living at high temperatures sufficient to dissociate a dimer.

The effects of temperature on binding of DHO by hDHOase and BcDHOase and subsequent catalysis have been compared. Table 1 shows that when hDHOase binds DHO (E + S → ES), there is a substantial release of enthalpy (−11.5 kcal/mol) and loss of entropy ($T\Delta S = -4.6$ kcal/

```
hamster    .......... .......... .......... .......... ..........
B.cal      .......... ....MGVWLK NGMSFNKDGE LMRTHIKIEH GTIAAILYEQ (36)

                                  * * * *
hamster    .........M TSQKLVRLPG LIDVHVHLRE PGGTHKEDFA SGTAAALAGG (41)
B.cal      PLEANEEDVI DVGGRLIVPG LIDLHVHLRE PGGEAKETIE TGTLAAAKGG (86)


hamster    VTMVCAMPNT RPPIIDAPAL ALAQKLAEAG ARCDFALFLG ASSENAG... (88)
B.cal      FTTVAAMPNT NPAPDRKEQM EWLQARIRET ARVNVLPYAA ITIGQKGEEL (136)


hamster    .......... ....TLGAVA GSAAGLKLYL NETFSELRLD SVAQWMEHFE (124)
B.cal      TDFAALKEAG AFAFTDDGVG VQSAGMMFEA MKQAAALDMA IVAHCEDDTL (186)

                                                              *
hamster    TWP..SHLPI VAHAE.RQSV AAVLMVAQLT Q......... RPVHICHVAR (162)
B.cal      TNGGAVHDGE FARRYGLRGI PSVCEAVHIA RDVLLAEAAG CHYHVCHIST (236)

                                     *
hamster    KEEILLIKTA KAQGLPVTCE VAPHHLFLNR EDLERLGPGR GEVRPELGSR (212)
B.cal      KESVRVVRDA KRAGIRVTAE VTPHHLLLCD EDIPGLDAN. YKMNPPLRSR (285)

                                  *   *   *
hamster    EDMEALWENM A..VIDCFAS DHAPHTLEEK ..CGPKPPPG FPGLETMLPL (258)
B.cal      EDRDALIEGL LDGTIDFIAT DHAPHTAAEK AKGIEAAPFG IVGLETAFPL (335)


hamster    ..LLTAVSEG RLSLDDLLQR LHHNPRRIFH LPL......Q EDTYVEVDLE (300)
B.cal      .LYTHFVKTG VFTLKQLVDW LTIKPAQCFG LKAGRLAVGA PADIAVIDLE (384)

           *
hamster    HEWTIPSHMP FSKARWTPFE GQKVKGTIRR VVLRGEVAYI DGQVL      (345)
B.cal      TEEAIDPETF ASKGKNTPFA GWVCQGWPVM TFVGGTLVWE KGRA.      (428)
```

FIGURE 7: Alignment of amino acid sequences for DHOases from hamster and *B. caldolyticus*. Conserved amino acids are shown in bold; those with an asterisk have been investigated by site-directed mutagenesis in hamster (*10*). The hamster DHOase sequence is for the core domain isolated after limited digestion with elastase (*13*). The two sequences show 32% identity and 43% homology.

mol), while BcDHOase releases a small amount of enthalpy (−4.2 kcal/mol) with a small increase in entropy ($T\Delta S$ = +1.4 kcal/mol). Decreases in entropy may result from the loss of rotational and translational entropies when DHO binds to DHOase or ordering of solvent water by a more highly charged ES complex (*21*, *22*). The substantial release of enthalpy observed on binding of DHO to hDHOase is consistent with formation of hydrogen and electrostatic bonds between the substrate and the active site leading to the electron shifts of catalysis (*23*, *24*). By contrast, for BcDHOase, the small release of enthalpy, small gain in entropy, and high $K_s$ value for DHO suggest formation of few bonds in a weakly interacting ES complex. Release of solvent molecules during formation of ES may make a positive entropy contribution augmented by less loss of rotational and translational entropies when DHO binds to BcDHOase. The thermodynamic data indicate different interactions for the transition from E + S → ES for hDHOase and BcDHOase.

As hDHOase and BcDHOase progress from the Michaelis complex to the transition-state complex (ES → ES$^{\ddagger}$), there is a further decrease in entropy (Table 1), consistent with increased polarity or some tightening of enzyme structure (*21*). Williams et al. (*10*) proposed that the polarized carbonyl at C6 of DHO is subject to nucleophilic attack by the zinc-bound hydroxyl ion forming a tetrahedral oxyanion transition state. We have subsequently shown that zinc-bound hydroxyl ion is not involved in initial substrate binding, but with the subsequent rate-determining step of catalysis (*25*). For hDHOase, the release of enthalpy (−11.5 kcal/mol, E + S → ES) is almost balanced by the enthalpy of activation (12.3 kcal/mol, ES → ES$^{\ddagger}$). The result is that in the temperature range 25−50 °C $k_{cat}/K_s$ is almost temperature independent ($\Delta H^{\ddagger}$ = 0.8 kcal/mol). A similar insensitivity of $k_{cat}/K_s$ to changing temperature has been reported for other enzymes, including cytidine deaminase (*26*), carbonic anhydrase II (*27*), lactate dehydrogenase (*28*), and ribonuclease A (*29*).

BcDHOase has enthalpies of activation (ES → ES$^{\ddagger}$) of 12.2 and 5.3 kcal/mol in the temperature ranges 30−50 and 50−70 °C, respectively. Biphasic plots of log($k_{cat}/T$) versus 1/$T$ (Figure 2) have also been observed for the Leu-Ile-Val binding protein from *E. coli* (*30*) and D-glyceraldehyde-3-phosphate dehydrogenase from *Methanothermus fervidus* (*31*), *Thermotoga maritima* (*32*), and *Thermoproteus tenax* (*33*). In the temperature range 30−50 °C, $k_{cat}/K_s$ is temperature dependent ($\Delta H^{\ddagger}$ = 8 kcal/mol). As the temperature increases above 50 °C, $k_{cat}/K_s$ becomes almost temperature independent ($\Delta H^{\ddagger}$ = 1.1 kcal/mol), suggesting that BcDHOase lowers the activation energy by forming a tighter transition-state complex at higher temperatures, which contributes to the greater loss of entropy. Above 50 °C, the thermophilic enzyme may channel vibrational energy more effectively into the substrate, driving it toward the transition state. This proposal is consistent with the natural environment of *B. caldolyticus*, where the enzyme has evolved to be catalytically efficient at high temperatures. The rigidity of thermophilic enzymes at 25 °C could restrict conformational changes required for catalytic function (*32*, *34*), explaining the low catalytic efficiency of BcDHOase at low temperatures. However, this low catalytic efficiency could equally be attributed to a local decrease in conformational flexibility.

The transition-state analogue, HDDP, binds more strongly to hDHOase than DHO, while HDDP binds marginally more

strongly to BcDHOase than DHO, and the affinity of BcDHOase for HDDP relative to DHO did not increase at elevated temperatures (Table 2). This result suggests some differences in the catalytic mechanisms of the two enzymes and possibly in the transition states. The amino acid sequences of hDHOase and BcDHOase (Figure 7) show 32% sequence identity and 43% homology for hamster DHOase without the 33 amino acid extension. The amino acid residues conserved with other species may be involved in substrate binding and catalysis, suggesting common aspects of the catalytic mechanism. Available structural data show that thermophilic proteins are strikingly similar to their mesophilic counterparts in their basic topology, activity, and catalytic mechanism (*35*).

Increasing temperature or urea concentration resulted in loss of DHOase activity due to unfolding of the protein indicated by the change in molar ellipticity. As expected, BcDHOase is more stable than the hDHOase with values for $T_m$ of 79.5 °C versus ~40 °C and $[urea]_{1/2}$ of 5.7 M versus ~3.8 M, respectively. The recombinant hamster DHOase, purified after limited digestion of CAD with elastase, gave a smooth unfolding transition centered at 45 °C with a smaller transition at 70 °C (*13*). By contrast, the recombinant hDHOase studied here did not give a definitive melting curve, possibly due to observed aggregation. The additional 33 amino acids required for recombinant expression of active hDHOase may induce precipitation during thermal unfolding. Comparison of the amino acid compositions of hDHOase and BcDHOase shows similar percentages of Pro, Asn, Gln, Met, and Cys, but BcDHOase has more Ile residues (6.08%) that could form clusters, compared with hDHOase (3.44%), that could contribute to the stability of BcDHOase. Circular dichroism spectra suggest that the content of α-helix for BcDHOase (50.5%) is higher than for hDHOase (39.8%), contributing to the stability of BcDHOase.

The results for the uncatalyzed hydrolysis of DHO yielded a linear Arrhenius plot (Figure 5) with an extrapolated rate constant of $3.2 \times 10^{-11}$ $s^{-1}$ at 25 °C. Extrapolation of the results of similar experiments conducted in other buffers (HCl, potassium [$^2$H]formate, phosphate, borate, or carbonate, 0.1 M) yielded values indicating that this reaction, like other reactions of carboxylic acid amides, is subject to specific acid and base catalysis but is uncatalyzed at pH 4 (Figure 6). We infer that the extrapolated rate constant of $3.2 \times 10^{-11}$ $s^{-1}$ at 25 °C represents the pseudo-first-order rate constant for water attack on DHO, with the activity of pure water taken as unity. The thermodynamics of activation for this reaction are $\Delta G^{\ddagger} = 30.7$ kcal/mol, $\Delta H^{\ddagger} = 24.7$ kcal/mol, and $T\Delta S^{\ddagger} = -6.9$ kcal/mol. Values of comparable magnitude have been recorded for the uncatatalyzed hydrolysis of similar bonds that join the elements of formamide, acetamide, *N*-methylacetamide, *N*,*N*-dimethylacetamide, urea, simple peptides, and the exocyclic amino group of cytidine (*36*).

Comparison of the kinetic constants for DHOase (Table 1), with this rate constant for the uncatalyzed hydrolysis of DHO, indicates that hDHOase enhances the rate of substrate hydrolysis by a factor of $1.6 \times 10^{14}$. The hamster enzyme achieves this rate enhancement almost entirely by lowering the enthalpy of activation ($\Delta\Delta H^{\ddagger} = -19.5$ kcal/mol), while the entropy of activation becomes only slightly more favorable ($T\Delta\Delta S^{\ddagger} = +2.3$ kcal/mol). That behavior, also observed for several other one-substrate and hydrolytic enzymes (*37*), implies that the rate enhancement and transition-state affinity of DHOase increase steeply with decreasing temperature. Evidently the increase in affinity, as the enzyme−substrate complex proceeds from the ground state to the transition state, is accompanied by a substantial release of enthalpy. That behavior is consistent with the development of new polar forces of attraction (H-bonds and electrostatic interactions) in the transition state that were not present in the enzyme−substrate complex in the ground state.

## CONCLUSIONS

DHO binds to hDHOase in the ground state with a low $K_s$ and a large release of enthalpy that could drive the substrate toward the transition state. The $k_{cat}/K_s$ value is relatively insensitive to temperature. BcDHOase binds DHO weakly with a high $K_s$ and small release of enthalpy. The decrease in activation energy for BcDHOase from 12.8 to 6.0 kcal/mol above 50 °C may be due to transition to a more active conformation. At high temperatures, BcDHOase acquires vibrational energy that could facilitate the transition $ES \rightarrow ES^{\ddagger}$, making the $k_{cat}/K_s$ values almost temperature independent. The rate enhancement for hydrolysis of DHO by hDHOase compared with the uncatalyzed reaction is a factor of $1.6 \times 10^{14}$.

## REFERENCES


1. Williams, N. K., Simpson, R. J., Moritz, R. L., Peide, Y., Crofts, L., Minasian, E., Leach, S. J., Wake, R. G., and Christopherson, R. I. (1990) Location of the dihydroorotase domain within trifunctional hamster dihydroorotate synthetase, *Gene 94*, 283−288.
2. Jones, M. E. (1980) Pyrimidine nucleotide biosynthesis in animals: genes, enzymes, and regulation of UMP biosynthesis, *Annu. Rev. Biochem. 49*, 253−279.
3. Simmer, J. P., Kelly, R. E., Rinker, A. G., Jr., Zimmermann, B. H., Scully, J. L., Kim, H., and Evans, D. R. (1990) Mammalian dihydroorotase: nucleotide sequence, peptide sequences, and evolution of the dihydroorotase domain of the multifunctional protein CAD, *Proc. Natl. Acad. Sci. U.S.A. 87*, 174−178.
4. Fields, C., Brichta, D., Shepherdson, M., Farinha, M., and O'Donovan, G. (1999) Phylogenetic analysis and classification of dihydroorotases: a complex history for a complex enzyme, *Paths Pyrimidines 7*, 49−62.
5. Kelly, R. E., Mally, M. I., and Evans, D. R. (1986) The dihydroorotase domain of the multifunctional protein CAD. Subunit structure, zinc content, and kinetics, *J. Biol. Chem. 261*, 6073−6083.
6. Martin, P. D., Purcarea, C., Zhang, P., Vaishnav, A., Sadecki, S., Guy-Evans, H. I., Evans, D. R., and Edwards, B. F. P. (2005) The crystal structure of a novel, latent dihydroorotase from *Aquifex aeolicus* at 1.7Å resolution, *J. Mol. Biol. 348*, 535−547.
7. Taylor, W. H., Taylor, M. L., Balch, W. E., and Gilchrist, P. S. (1976) Purification and properties of dihydroorotase, a zinc-containing metalloenzyme in *Clostridium oroticum*, *J. Bacteriol. 127*, 863−873.
8. Thoden, J. B., Phillips, G. N. J., Neal, T. M., Raushel, F. M., and Holden, H. M. (2001) Molecular structure of dihydroorotase: a paradigm for catalysis through the use of a binuclear metal center, *Biochemistry 40*, 6989−6997.
9. Lee, M., Chan, C. W., Guss, J. M., Christopherson, R. I., and Maher, M. J. (2005) Dihydroorotase from *Escherichia coli:* loop movement and cooperativity between subunits, *J. Mol. Biol. 348*, 523−533.
10. Williams, N. K., Manthey, M. K., Hambley, T. W., O'Donoghue, S. I., Keegan, M., Chapman, B. E., and Christopherson, R. I. (1995) Catalysis by hamster dihydroorotase: zinc binding, site-directed mutagenesis, and interaction with inhibitors, *Biochemistry 34*, 11344−11352.
11. Christopherson, R. I., and Jones, M. E. (1980) The effects of pH and inhibitors upon the catalytic activity of the dihydroorotase of

multienzymatic protein pyr1−3 from mouse Ehrlich ascites carcinoma, *J. Biol. Chem. 255*, 3358−3370.
12. Ghim, S. Y., Nielsen, P., and Neuhard, J. (1994) Molecular characterization of pyrimidine biosynthesis genes from the thermophile *Bacillus caldolyticus*, *Microbiology 140*, 479−491.
13. Hemmens, B., and Carrey, E. A. (1995) Mammalian dihydroorotase; secondary structure, and interactions with other proteolytic fragments from the multienzyme polypeptide CAD, *Eur. J. Biochem. 231*, 220−225.
14. Pace, C. N., and Scholtz, M. (1997) in *Protein function: a practical approach* (Creighton, T. E., Ed.) pp 299−321, Oxford University Press, Oxford, New York.
15. Christopherson, R. I., Schmalzl, K. J., Szabados, E., Goodridge, R. J., Harsanyi, M. C., Sant, M. E., Algar, E. M., Anderson, J. E., Armstrong, A., and Sharma, S. C. (1989) Mercaptan and dicarboxylate inhibitors of hamster dihydroorotase, *Biochemistry 28*, 463−470.
16. Washabaugh, M. W., and Collins, K. D. (1984) Dihydroorotase from *Escherichia coli*. Purification and characterization, *J. Biol. Chem. 259*, 3293−3298.
17. Pettigrew, D. W., Bidigare, R. R., Mehta, B. J., Williams, M. I., and Sander, E. G. (1985) Dihydro-orotase from *Clostridium oroticum.* Purification and reversible removal of essential zinc, *Biochem. J. 230*, 101−108.
18. Ogawa, J., and Shimizu, S. (1995) Purification and characterization of dihydroorotase from *Pseudomonas putida*, *Arch. Microbiol. 164*, 353−357.
19. Krungkrai, J., Cerami, A., and Henderson, G. B. (1990) Pyrimidine biosynthesis in parasitic protozoa: purification of a monofunctional dihydroorotase from *Plasmodium berghei* and *Crithidia fasciculata*, *Biochemistry 29*, 6270−6275.
20. Washabaugh, M. W., and Collins, K. D. (1986) Dihydroorotase from *Escherichia coli*. Sulfhydryl group-metal ion interactions, *J. Biol. Chem. 261*, 5920−5929.
21. Laidler, K. J., and Peterman, B. F. (1979) Temperature effects in enzyme kinetics, *Methods Enzymol. 63*, 234−257.
22. Fersht, A. (1977) *Enzyme Structure and Mechanism*, Freeman, New York.
23. Schramm, V. L. (1998) Enzymatic transition states and transition state analogue design, *Annu. Rev. Biochem. 67*, 693−720.
24. Cleland, W. W., and Northrop, D. B. (1999) Energetics of substrate binding, catalysis, and product release, *Methods Enzymol. 308*, 3−27.
25. Huang, D. T., Thomas, M. A., and Christopherson, R. I. (1999) Divalent metal derivatives of the hamster dihydroorotase domain, *Biochemistry 38*, 9964−9970.
26. Snider, M. J., Gaunitz, S., Ridgway, C., Short, S. A., and Wolfenden, R. (2000) Temperature effects on the catalytic efficiency, rate enhancement, and transition state affinity of cytidine deaminase, and the thermodynamic consequences for catalysis of removing a substrate "anchor", *Biochemistry 39*, 9746−9753.
27. Ghannam, A. F., Tsen, W., and Rowlett, R. S. (1986) Activation parameters for the carbonic anhydrase II-catalyzed hydration of $CO_2$, *J. Biol. Chem. 261*, 1164−1169.
28. Borgmann, U., Moon, T. W., and Laidler, K. J. (1974) Molecular kinetics of beef heart lactate dehydrogenase, *Biochemistry 13*, 5152−5158.
29. Eftink, M. R., and Biltonen, R. L. (1983) Energetics of ribonuclease A catalysis. 3. Temperature dependence of the hydrolysis of cytidine cyclic 2′,3′-phosphate, *Biochemistry 22*, 5140−5150.
30. Gaudin, C., Marty, B., Ragot, M., Sari, J. C., and Belaich, J. P. (1980) Thermodynamic studies of binding proteins: effects of temperature variations on substrate binding and conformation of the leucine-isoleucine-valine binding protein of *Escherichia coli*, *Biochimie 62*, 741−746.
31. Fabry, S., and Hensel, R. (1987) Purification and characterization of D-glyceraldehyde-3-phosphate dehydrogenase from the thermophilic archaebacterium *Methanothermus fervidus*, *Eur. J. Biochem. 165*, 147−155.
32. Wrba, A., Schweiger, A., Schultes, V., Jaenicke, R., and Zavodsky, P. (1990) Extremely thermostable D-glyceraldehyde-3-phosphate dehydrogenase from the eubacterium *Thermotoga maritima*, *Biochemistry 29*, 7584−7592.
33. Hensel, R., Laumann, S., Lang, J., Heumann, H., and Lottspeich, F. (1987) Characterization of two D-glyceraldehyde-3-phosphate dehydrogenases from the extremely thermophilic archaebacterium *Thermoproteus tenax*, *Eur. J. Biochem. 170*, 325−333.
34. Zavodszky, P., Kardos, J., Svingor, and Petsko, G. A. (1998) Adjustment of conformational flexibility is a key event in the thermal adaptation of proteins, *Proc. Natl. Acad. Sci. U.S.A. 95*, 7406−7411.
35. Jaenicke, R. (1991) Protein stability and molecular adaptation to extreme conditions, *Eur. J. Biochem. 202*, 715−728.
36. Callahan, B. P., Yuan, Y., and Wolfenden, R. (2005) The burden borne by urease, *J. Am. Chem. Soc. 127*, 10828−10829.
37. Wolfenden, R., Sinder, M., Ridgway, C., and Miller, B. (1999) The temperature dependence of enzyme rate enhancements, *J. Am. Chem. Soc. 121*, 7419−7420.
38. Williams, N. K., Peide, Y., Seymour, K. K., Ralston, G. B., and Christopherson, R. I. (1993) Expression of catalytically active hamster dihydroorotase domain in *Escherichia coli:* purification and characterization, *Protein Eng. 6*, 333−340.
39. Riddles, P. W., Blakeley, R. L., and Zerner, B. (1983) Reassessment of Ellman's reagent, *Methods Enzymol. 91*, 49−60.
40. Segal, I. H. (1975) *Enzyme Kinetics: Behaviour and Analysis of Rapid Equilibrium and Steady-State Enzyme Systems*, Wiley, New York.

BI060595W